Published in final edited form as:
Circulation. 2008 August 19; 118(8): 845–852. doi:10.1161/CIRCULATIONAHA.107.749440.

Mitral Leaflet Adaptation to Ventricular Remodeling Occurrence and Adequacy in Patients With Functional Mitral Regurgitation

Miguel Chaput, MD, **Mark D. Handschumacher, BS**, **Francois Tournoux, MD**, **Lanqi Hua, RDCS**, **J. Luis Guerrero, BS**, **Gus J. Vlahakes, MD**, and **Robert A. Levine, MD**
From the Division of Cardiothoracic Surgery and Cardiac Ultrasound Laboratory, Massachusetts General Hospital, Harvard Medical School, Boston, Mass.

Abstract

Background—Functional mitral regurgitation (MR) is caused by systolic traction on the mitral leaflets related to ventricular distortion. Little is known about whether chronic tethering causes the mitral leaflet area to adapt to the geometric needs imposed by tethering, in part because of inability to reconstruct leaflet area in vivo. Our aim was to explore whether adaptive increases in leaflet area occur in patients with functional MR compared with normal subjects and to test the hypothesis that leaflet area influences MR severity.

Methods and Results—A new method for 3-dimensional echocardiographic measurement of mitral leaflet area was developed and validated in vivo against 15 sheep heart valves, later excised. This method was then applied in 80 consecutive patients from 3 groups: patients with normal hearts by echocardiography (n=20), patients with functional MR caused by isolated inferior wall-motion abnormality or dilated cardiomyopathy (n=29), and patients with inferior wall-motion abnormality or dilated cardiomyopathy but no MR (n=31). Leaflet area was increased by 35±20% in patients with LV dysfunction compared with normal subjects. The ratio of leaflet to annular area was 1.95±0.40 and was not different among groups, which indicates a surplus leaflet area that adapts to left-heart changes. In contrast, the ratio of total leaflet area to the area required to close the orifice in midsystole was decreased in patients with functional MR compared with those with normal hearts (1.29±0.15 versus 1.78±0.39, P=0.001) and compared with patients with inferior wall-motion abnormality or dilated cardiomyopathy but no MR (1.81±0.38, P=0.001). After adjustment for measures of LV remodeling and tethering, a leaflet-to-closure area ratio <1.7 was associated with significant MR (odds ratio 23.2, 95% confidence interval 2.0 to 49.1, P=0.02).

Conclusions—Mitral leaflet area increases in response to chronic tethering in patients with inferior wall-motion abnormality and dilated cardiomyopathy, but the development of significant MR is associated with insufficient leaflet area relative to that demanded by tethering geometry. The varying adequacy of leaflet adaptation may explain in part the heterogeneity of this disease among patients. The results suggest the need to understand the mechanisms that underlie leaflet adaptation and whether leaflet area can potentially be modified as part of the therapeutic approach.

Keywords

regurgitation; heart failure; echocardiography; mitral valve; valves

Correspondence to Robert A. Levine, MD, Massachusetts General Hospital, Yawkey-5068, 55 Fruit St, Boston, MA, 02114. E-mail rlevine@ partners.org.

The online-only Data Supplement is available with this article at http://circ.ahajournals.org/cgi/content/full/CIRCULATIONAHA.107.749440/DC1

Disclosures
None.

Functional mitral regurgitation (FMR) is a frequent complication of coronary artery disease and dilated cardiomyopathy (DCM) that doubles late mortality.[1–4] It is caused by left ventricular (LV) distortion, which leads to displacement of the papillary muscles.[5–12] This translates into increased tension on the mitral leaflets during systole, which tethers them below the annulus and impairs coaptation. It is reasonable to expect that mitral leaflet size can play an important role in determining whether mitral regurgitation (MR) actually develops when the leaflets are tethered, but this is as yet unexplored. Little is also known about adaptation of the mitral leaflets to LV remodeling.

Mitral leaflets are acutely distensible, and their stress-strain relationship has been described in vitro,[13,14] with increases of up to 15% in length under physiological tension; leaflet size reverts to normal when tension is released. It is unknown, however, whether chronic tension leads to permanent increases in size, as it does in bone, vessels, and skin.[15–17] Leaflet lengthening, mainly near the edge, has recently been described in a heart failure model at end systole, when passive stretch may be superimposed on actual leaflet growth.[18] Decreased distensibility of explanted leaflets has been described in patients with severe heart failure,[19, 20] although this has not been correlated with total leaflet area.

FMR is often associated with annular dilatation, which necessarily increases leaflet circumference. Whether this is associated with changes in total leaflet area as an adaptation to chronic tethering that could reduce FMR is not known. In part, this reflects the lack of an imaging technique for measuring mitral leaflet area and its adaptation to changes in the LV.

Our aim was to explore the relationship between leaflet adaptation and the development of MR in the spectrum of patients who present with FMR, which is typically associated with either isolated inferior wall-motion abnormality (IWMA) or DCM. To achieve this goal, we developed a technique for measuring mitral leaflet area in vivo using 3-dimensional (3D) echocardiography. We validated this technique in an animal model and then applied it in patients with FMR to address the hypothesis that leaflet adaptation occurs in patients with chronic tethering but is insufficient to meet the needs for leaflet area imposed by tethering, along with the corollary that leaflet area contributes to the degree of MR.

Methods

Validation Studies

Fifteen healthy Dorsett hybrid sheep were studied by epicardial echocardiography. An apical full-volume data set was acquired over 4 beats with an iE33 3D echocardiography scanner (Philips, Andover, Mass). Animals were euthanized, and the valve was explanted and unfurled on millimetric paper with minimal tension (Figure 1). The valve was traced and photographed, and its area was measured with graphics software (Adobe Photoshop 8.0, Adobe Systems Inc, New York, NY). This study was approved by the local committee on animal care (Institutional Animal Care and Use Committee).

Patient Population

From the out-patient and in-patient lists of the Cardiac Ultrasound Laboratory at our institution, 84 consecutive patients were prospectively recruited after they provided informed consent. Inclusion criteria included a normal heart (n=24), isolated IWMA (n=30), and global LV dysfunction (ejection fraction <35%) with LV dilatation, defined by a subvalvular end-diastolic diameter >60 mm in the parasternal long-axis view (DCM; n=30). Patients with mitral prolapse, endocarditis, and aortic valve disease were excluded. Four patients were excluded owing to poor image quality, all in the normal group with nondilated LVs and more limited imaging

windows, and the remaining 80 patients constituted the study group (normal, n=20; IWMA, n=30; and DCM, n=30).

To analyze the determinants of FMR, study patients were characterized as having important MR (moderate or greater), defined by a proximal jet width ≥4 mm in the apical long-axis view[21,22] (FMR group, n=29; 16 with IWMA, 13 with DCM) or no important MR (no MR to mild MR, n=31; 14 with IWMA, 17 with DCM). Two patients with DCM had atrial fibrillation and were included in the study. The study was approved by the hospital's institutional review board.

Echocardiography

Basic views were obtained with a Philips iE33 scanner and a 5-MHz transducer. Images were analyzed offline with QLab 5.1 (Philips). LV end-diastolic volume, end-systolic volume, and ejection fraction were measured by the biplane Simpson technique. MR was quantified by the width of the proximal jet (vena contracta) in the apical long-axis view.[21,22] Tethering distance was assessed in an apical 2-chamber view as the distance between the posterior papillary muscle tip and the contralateral annulus, as described previously.[8,23] Leaflet length was measured by 2-dimensional echo from leaflet insertion to tip in the parasternal long-axis view during diastasis before end diastole. Anterior and posterior leaflet thicknesses were measured in the 4-chamber view in the midleaflet at end diastole to minimize the impact of stretch.

Mitral Annulus and Leaflet Surface Area

Images were obtained with an X3 matrix-array transducer (Philips) to acquire 3D volumetric data sets of the mitral valve from 4 heart beats. Leaflet areas were analyzed in midsystole and end diastole with custom software running on a personal computer (Omni4D, M.D.H.). Total leaflet area can be measured clearly only in diastole, because in systole, the area of each leaflet involved in coaptation cannot be visualized uniformly. Measurement of the diastolic leaflet area also evaluates adaptation when LV pressure and leaflet tension are minimal, without the effects of passive systolic stretch. Therefore, total leaflet area was assessed at full end-diastolic leaflet opening, 1 frame before closure motion.

Three-Dimensional Tracing

First, an anatomic reference frame was used to derive a set of views through the mitral valve rotated around an axis that passed from the LV apex through the center of the mitral annulus.[24] Tracing was simplified by automatic computation of a set of 9 equiangular image planes (0° to 180°) that intersected this axis, with the 0° view passing through the center of the aortic valve (Figure 1). The annular points, leaflets, and open leaflet tips were traced manually with different colors for identification on the image planes, which provided 2 leaflet traces per plane for a total of 18 traces. Leaflet tips were identified as the end of the relatively thick and continuous-appearing leaflet bodies, assisted by visualization of the valve in cine loop.

An automated computer algorithm connected the individual annular points to form a closed, 3D annular loop and then computed an open, tubelike 3D polygonal surface that conformed to the leaflet traces (Figure 2, left; online-only Data Supplement Appendix). Leaflet area was calculated by summing the elements of this 3D polygonal surface.

In midsystole, the closed leaflet surface was computed to provide the closure area as the minimal area of the leaflets necessary to occlude the orifice on the basis of their 3D shape, which is dictated by leaflet tethering.[24] The closure area was measured as a continuous surface area separating the left atrial and LV cavities (Figure 2, right; online-only Data Supplement Appendix); this measurement excludes the juxtaposed leaflet surface portions that meet in systole but do not separate the 2 cavities. The regurgitant orifice itself is not visualized directly

and therefore is not excluded from this area; the closure area is thus the area necessary for the leaflets to completely close the orifice between the 2 cavities. The normal surplus of leaflet area translates into a total leaflet area–to-closure area ratio well above 1.[25] Finally, mitral annular area was calculated as the projection of the annular trace onto its average or least-squares plane.[24]

To test whether leaflet area increased relative to changes in the left side of the heart, we calculated the ratio of leaflet to annular area, both in diastole. To assess the adequacy of leaflet compensation, we calculated the ratio of total leaflet area to leaflet closure area.

Statistical Analysis

Measurements of leaflet size (area, length, and thickness) were made by an observer who was blind to the patient's group (presence or absence of FMR not seen on 3D leaflet acquisitions). Valve area and lengths were consistently measured by 1 physician with advanced echocardiographic training, and variability was compared with another comparably trained physician; both were experienced with 3D echocardiographic navigation and with the software. Leaflet thickness was consistently measured by 1 cardiac sonographer with 10 years experience.[26]

Validation of the leaflet area measurement was performed by linear regression between anatomic ex vivo measurements and echocardiographic measurements; agreement was assessed by Bland-Altman analysis and paired *t* test. Intraobserver and interobserver (2 independent readers) variability was also assessed by Bland-Altman analysis. In addition, interobserver variability was measured by κ-coefficient between the 2 readers. For continuous variables, patient groups were compared with 1-way ANOVA and, for pairwise comparisons, Student-Newman-Keuls tests. A linear regression model to explain variations in MR by proximal jet width was built with LV end-systolic volume, LV ejection fraction, annular area, leaflet area–to–annular area ratio, tethering distance, and patient age. Those variables were chosen from the univariate analysis for the prediction of MR proximal jet width. Finally, a logistic regression model was built to predict the development of important (moderate or more) MR (proximal jet width ≥4 mm) based on dichotomized variables: LV dilatation (end-systolic volume >80 mL), LV dysfunction (ejection fraction <35%), annular dilatation (projected annulus at end systole >9.0 cm^2), tethering distance >3.8 cm, and low leaflet-to–closure area ratio (<1.7). These thresholds were chosen from observation of the frequency of important MR along the distribution of the predicting variables, with identification of natural cutoffs, and because of their association with FMR on the basis of widely accepted criteria and a literature search (tethering distance). [8,23] Analyses were performed with SAS 9.1 (SAS Institute, Cary, NC). Values are reported as mean± SD.

The authors had full access to and take full responsibility for the integrity of the data. All authors have read and agree to the manuscript as written.

Results

Validation Studies

Correlation between anatomic measurements and echocardiography-derived leaflet area is shown in Figure 3 (R^2=0.86, P<0.0001, SEE=1.24). Differences from anatomic data were not significantly different from 0 (mean residual 0.51 ± 1.15, P=0.71). The average residual was −0.13±0.51 (P=0.85 versus 0) for intraobserver variability and 0.24 ± 1.10 (P=0.79 versus 0) for interobserver variability. The κ-value was 0.78, which suggests high interrater correlation.

Patient Population

Patient characteristics are shown in Table 1. No significant age difference was found among groups. Ejection fraction was significantly lower and LV volumes and annular area were higher in all disease groups compared with the group with normal hearts. Annular area increased by 29 ± 5% (P=0.003) in patients with important MR and by 21 ± 6% (P=0.01) in patients without MR compared with the normal group.

Leaflet Area and LV Remodeling

Total leaflet area increased by 32.5 ± 19.2% (P<0.0001) in patients with important (moderate or more) MR (pooled IWMA and DCM) versus normal hearts and by 37.5 ± 21.0% (P<0.0001) in patients with LV abnormalities but without significant MR (no MR to mild MR, P=0.9 versus MR; Figure 4). Leaflet area likewise increased when normalized to body surface area in patients with left-heart disease compared with normal hearts (normal 8.3 ± 1.6 cm^2/m^2, FMR 10.5 ± 2.2 cm^2/m^2, P=0.001; LV abnormalities but no important FMR 9.8 ± 1.9 cm^2/m^2, P=0.03 versus normal).

In patients with DCM, patients without MR had larger leaflet areas than those having MR (DCM but no MR 22.2 ± 2.0 cm^2, DCM plus MR 20.2 ± 2.3 cm^2, P=0.03); no significant differences in LV ejection fraction or volumes were found between DCM patients with and those without MR. Leaflet thickness was increased from normal in all disease groups except for patients with IWMA but no MR (Table 2). In patients with IWMA, although leaflet area was not significantly different in patients with and without MR (Table 2), those with MR had a lower ejection fraction (35 ± 7% versus 42 ± 7%, P=0.05), higher end-systolic volume (95 ± 23 versus 77 ± 20 mL, P=0.05), and larger annular area (P<0.05), which indicated greater LV remodeling. In contrast to leaflet area, anterior and posterior leaflet 2-dimensional lengths were not significantly different in patients with IWMA and DCM, whether MR was present or not.

Systolic leaflet closure area was increased in all LV dysfunction patients with and without MR compared with those with normal hearts, which indicated significant tethering (normal 8.6 ± 1.7 cm^2, FMR 15.3 ± 2.7 cm^2, P<0.0001, no important MR 10.8 ± 2.4 cm^2, P=0.01 versus normal). Closure area was significantly higher in patients with FMR than in patients with LV abnormalities but without important FMR (1.92 ± 0.40 cm^2 versus 1.10 ± 0.45 cm^2, P=0.0005).

As shown in Figure 5, the leaflet-to–annular area ratio was similar in all groups, including normal patients, maintaining a relatively constant ratio of 1.95 ± 0.24. This suggests that leaflet adaptation correlates with annular dilatation. In contrast, the leaflet-to–closure area ratio was strongly decreased in patients with MR (1.29 ± 0.15 versus 1.78 ± 0.39, P=0.0001) but not in patients with LV disease but no MR (1.81 ± 0.38), which suggests sufficient adaptation to chronic tethering in patients without MR but incomplete adaptation in patients who develop MR.

Linear and Logistic Regression Models

When adjusted for LV size, LV function, annular area, tethering distance, and patient age, the ratio of leaflet to closure area was a significant predictor of MR severity by proximal jet width (linear regression r^2=0.93, b=0.19, P=0.04). As shown in Table 3, all dichotomized variables included in the multiple variable logistic regression model were significantly associated with the development of important MR by univariate analysis. A leaflet-to–closure area ratio less than 1.7 independently predicted the presence of moderate to severe MR (odds ratio 23.2, 95% confidence interval 2.0 to 49.1, P=0.02) after adjustment for dilated LV, poor LV function, dilated annulus in midsystole, tethering length, and type of disease (DCM versus IWMA).

Discussion

Given that FMR is caused by leaflet tethering to displaced papillary muscle and annular attachments, variation in leaflet size may be an important determinant of whether the valve is actually insufficient. Anatomists have long taught that the mitral valve has a substantial surplus in area relative to the annular orifice, which allows the heart to adapt to volume overload without developing MR.[25,27,28] In LV dysfunction, however, the leaflet surface is displaced below the annulus, which increases the closure area necessary to prevent regurgitation. It has been suggested that in this condition, the leaflets may elongate in response to the stresses imposed by increased tethering.[19,20] Surprisingly, however, little is known about such proposed elongation.

Until now, noninvasive methods have not been available to address this question of leaflet adaptation in vivo. This would be required not only to measure total leaflet area in situ without extraneous stretch but especially to relate total area to the closed systolic surface area of the tethered leaflets and to the degree of MR, which can only be measured in vivo. Therefore, we developed an algorithm for reconstructing leaflet area by real-time 3D echocardiography and validated it against excised specimens. This method for the first time allowed measurement of leaflet area in the beating heart under physiological loads.

This algorithm was then applied in patients with the classic scenarios in which FMR develops, segmental inferior-wall and global LV dysfunction. The results showed that mitral leaflet area does increase by up to 35% on average in patients with IWMA and DCM compared with normal subjects. This degree of leaflet area augmentation exceeds that which can be explained by passive stretching of the valve,[13] and moreover, it is measured in the unstretched leaflets during diastole. Interestingly, the ratio of leaflet to annular cross-sectional area was relatively constant among patients and normal subjects; this suggests that the valve enlarges predominantly through expansion of its annular circumference rather than by elongation from insertion to tip. These lengths, measured through the center of the valve in a long-axis view, were not different among patient groups and normal subjects for either leaflet (Table 2), which contributes to the visual impression of lack of adaptation based on 2-dimensional images in clinical experience.[19]

On the other hand, this leaflet area adaptation is often insufficient to meet the need for an expanded leaflet closure surface demanded by the tethered leaflet geometry. The normal surplus of leaflet relative to the closure area is substantially smaller in patients with FMR, which allows greater opportunities for insufficiency (Figure 5). The regression analysis further shows that variation in leaflet area relative to closure area independently contributes to variation in the degree of MR, so that patients with relatively larger leaflets have less MR.

The nearly 2-fold leaflet surplus relative to annular area in the present study is comparable to that described anatomically by Chiechi et al.[25] Although Hueb et al[29] also described increased leaflet area in autopsy specimens of patients with FMR, their values were roughly 50% of those described in vivo, which was possibly related to valve fixation, but their values were also roughly equivalent to the annular area, as opposed to the normal nearly 2-fold surplus, because they photographically measured the projected leaflet area viewed through the annulus as opposed to planimetering the excised leaflet area. Measurement of excised areas cannot relate leaflet area to the systolic leaflet closure area (which requires the in situ tethered leaflet geometry) or to the degree of MR, both of which were quantified in the present in vivo study.

These data raise intriguing questions about valve biology. Recognition is growing that the cardiac valves are not passive tissue flaps but are capable of active remodeling. Transition of endothelial to mesenchymal progenitor cells can be induced by growth factors, which leads to elaboration of extracellular matrix.[30–36] Apoptosis and matrix degradation by

metalloproteinases curtail valve growth. How valve plasticity is affected by the tethering stresses is currently unknown, although increased valve stiffness and decreased extensibility have been described in patients with end-stage heart failure, whose mitral valves are biochemically different, with increased collagen and glycosaminoglycan concentrations,[19, 20] as in other valves subjected to altered stress.[37–39] Increased aortic leaflet size has likewise been described in patients with aortic root dilatation and aortic insufficiency.[40] Adaptation coincides with known increases in collagen production and transforming growth factor-β secretion with cyclic stretch of aortic valve interstitial cells.[41] The present data provide a rationale and context for exploring the basic mechanisms of valve growth and its limitations, which have clear therapeutic implications. The possibility of surgical leaflet elongation has been raised by other groups[42–44] and is also being explored.

Limitations and Future Directions

In the present study, we measured total leaflet area in diastole. Although total systolic leaflet area would also have been of interest, the inability to measure the coapted leaflet portions unambiguously where the leaflets are juxtaposed limits this measurement.

The diastolic, open leaflet area, however, has the advantage of providing a measure of long-term leaflet adaptation without the superimposed effects of systolic stretch.[45] The observation of fairly constant diastolic leaflet length also indicates that we are measuring long-term adaptation of leaflet size as opposed to a short-term stretch, which predominantly increases leaflet length.[13] Three-dimensional echocardiography has recognized limitations of spatial and temporal resolution. Careful review of cine loops in multiple imaging planes perpendicular to the annulus helped define the annular hinge points. The accuracy of any surfacing algorithm is subject to the size of the mesh elements and the degree of smoothing. Trace irregularity can increase calculated area relative to actual area. To minimize this effect after the initial tracing, the 3D reconstruction of the valve was reviewed carefully for consistency; also, the algorithm for modeling the wire mesh surface used a distance-weighted averaging of neighboring points to avoid sharp angular changes of adjacent tiles that would overestimate the surface area.

Of note is that the increase in leaflet area compared with normal hearts was comparable in patients with localized versus global LV dysfunction, despite typical differences in LV size in those 2 groups. Thus, leaflet area increase cannot simply be ascribed to global LV dilatation but relates more closely to localized tethering and annular changes.

In summary, therefore, mitral leaflet area undergoes long-term adaptation in states of LV dysfunction in parallel with annular area, but in patients with FMR, such adaptation is insufficient to meet the needs for increased leaflet area imposed by the tethered leaflet configuration. Furthermore, variation in leaflet area in relation to the required closure area is an important determinant of the degree of MR. Finally, the results suggest the need to understand the mechanisms that underlie leaflet adaptation and whether leaflet area can potentially be modified as part of the therapeutic approach to FMR.

CLINICAL PERSPECTIVE

Left ventricular remodeling after myocardial infarction or in dilated cardiomyopathy creates mismatch between mitral leaflet and ventricular size, which leads to ischemic mitral regurgitation, a source of increased heart failure and mortality. We explored whether the valve itself adapts to the stresses imposed by the dilating ventricle. Three-dimensional echocardiography, validated against excised valves, measured diastolic leaflet area in 80 patients and control subjects. Leaflet area was an average of 35% greater in patients with left ventricular dysfunction than in control subjects. Leaflet area showed comparable adaptation to annular area in all groups (nearly 2-fold ratio). However, leaflet area was a

strong independent predictor of mitral regurgitation, and patients with mitral regurgitation had reduced ratios of total leaflet area to the tented leaflet area required to close the annular orifice in systole. The valve therefore adapts to the increased size of remodeled ventricles, but the degree of adaptation may be insufficient to prevent mitral regurgitation by meeting the geometric demands imposed on the stretched leaflets. Understanding the mechanisms of mitral valve adaptation can potentially provide new therapeutic targets.

Acknowledgment

We thank Shirley Sims for her expert editorial assistance.

Sources of Funding

This study was supported by grant 07CVD04 from the Fondation Leducq, Paris, France, for the Transatlantic MITRAL Network of Excellence, and by grants R01 HL38176 and K24 HL67434 of the National Institutes of Health, Bethesda, Md.

References

1. Grigioni F, Enriquez-Sarano M, Zehr KJ, Bailey KR, Tajik AJ. Ischemic mitral regurgitation: long-term outcome and prognostic implications with quantitative Doppler assessment. Circulation 2001;103:1759–1764. [PubMed: 11282907]
2. Lamas GA, Mitchell GF, Flaker GC, Smith SC Jr, Gersh BJ, Basta L, Moye L, Braunwald E, Pfeffer MA. Clinical significance of mitral regurgitation after acute myocardial infarction. Circulation 1997;96:827–833. [PubMed: 9264489]
3. Barzilai B, Gessler C, Perez JE, Schaab C, Jaffe AS. Significance of Doppler-detected mitral regurgitation in acute myocardial infarction. Am J Cardiol 1988;61:220–223. [PubMed: 3341197]
4. Feinberg MS, Schwammenthal E, Shlizerman L, Porter A, Hod H, Freimark D, Matezky S, Boyko V, Mandelzweig L, Vered Z. Prognostic significance of mild mitral regurgitation by color Doppler echocardiography in acute myocardial infarction. Am J Cardiol 2000;86:903–907. [PubMed: 11053696]
5. Ogawa S, Hubbard FE, Mardelli TJ, Dreifus LS. Cross-sectional echo-cardiographic spectrum of papillary muscle dysfunction. Am Heart J 1979;97:312–321. [PubMed: 420070]
6. Godley RW, Wann LS, Rogers EW, Feigenbaum H, Weyman AE. Incomplete mitral leaflet closure in patients with papillary muscle dysfunction. Circulation 1981;63:565–571. [PubMed: 7460242]
7. Sabbah HN, Kono T, Rosman H, Jafri S, Stein PD, Goldstein S. Left ventricular shape: a factor in the etiology of functional mitral regurgitation in heart failure. Am Heart J 1992;123(part 1):961–966. [PubMed: 1532283]
8. Otsuji Y, Handschumacher MD, Schwammenthal E, Jiang L, Song J-K, Guerrero JL, Vlahakes GJ, Levine RA. Insights from three-dimensional echocardiography into the mechanism of functional mitral regurgitation: direct in vivo demonstration of altered leaflet tethering geometry. Circulation 1997;96:1999–2008. [PubMed: 9323092]
9. He S, Fontaine AA, Schwammenthal E, Yoganathan AP, Levine RA. Integrated mechanism for functional mitral regurgitation: leaflet restriction versus coapting force: in vitro studies. Circulation 1997;96:1826–1834. [PubMed: 9323068]
10. Komeda M, Glasson JR, Bolger AF, Daughters GTI, Ingels NB Jr, Miller DC. Papillary muscle-left ventricular wall “complex”. J Thorac Cardiovasc Surg 1997;113:292–301. [PubMed: 9040623]
11. Llaneras MR, Nance ML, Streicher JT, Linden PL, Downing SW, Lima JA, Deac R, Edmunds LH Jr. Pathogenesis of ischemic mitral insufficiency. J Thorac Cardiovasc Surg 1993;105:439–442. [PubMed: 8445923]
12. Yiu SF, Enriquez-Sarano M, Tribouilloy C, Seward JB, Tajik AJ. Determinants of the degree of functional mitral regurgitation in patients with systolic left ventricular dysfunction: a quantitative clinical study. Circulation 2000;102:1400–1406. [PubMed: 10993859]
13. May-Newman K, Yin FC. Biaxial mechanical behavior of excised porcine mitral valve leaflets. Am J Physiol Heart Circ Physiol 1995;269:H1319–H1327.

14. Kunzelman KS, Cochran RP. Stress/strain characteristics of porcine mitral valve tissue: parallel versus perpendicular collagen orientation. J Card Surg 1993;7:71–78. [PubMed: 1554980]
15. Gosain AK, Song LS, Santoro T, Weihrauch D, Bosi BO, Corrao MA, Chilian WM. Effects of transforming growth factor-beta and mechanical strain on osteoblast cell counts: an in vitro model for distraction osteogenesis. Plast Reconstr Surg 2000;105:130–136. [PubMed: 10626981]
16. De Filippo R, Atala A. Stretch and growth: the molecular and physiologic influences of tissue expansion. Plast Reconstr Surg 2002;109:2450–2462. [PubMed: 12045576]
17. Davis NP, Han H-C, Wayman B, Vito R. Sustained axial loading lengthens arteries in organ culture. Ann Biomed Eng 2005;33:867–877. [PubMed: 16060526]
18. Timek TA, Lai DT, Dagum P, Liang D, Daughters GT, Ingels NB Jr, Miller DC. Mitral leaflet remodeling in dilated cardiomyopathy. Circulation 2006;114(Suppl I):I-518–I-523. [PubMed: 16820630]
19. Grande-Allen KJ, Borowski AG, Troughton RW, Houghtaling PL, DiPaola NR, Moravec CS, Vesely I, Griffin BP. Apparently normal mitral valves in patients with heart failure demonstrate biochemical and structural derangements: an extracellular matrix and echocardiographic study. J Am Coll Cardiol 2005;45:54–61. [PubMed: 15629373]
20. Grande-Allen KJ, Barber JE, Klatka KM, Houghtaling PL, Vesely I, Moravec CS, McCarthy PM. Mitral valve stiffening in end-stage heart failure: evidence of an organic contribution to functional mitral regurgitation. J Thorac Cardiovasc Surg 2005;130:783–790. [PubMed: 16153929]
21. Mele D, Vandervoort P, Palacios I, Rivera JM, Dinsmore RE, Schwammenthal E, Marshall JE, Weyman AE, Levine RA. Proximal jet size by Doppler color flow mapping predicts severity of mitral regurgitation: clinical studies. Circulation 1995;91:746–754. [PubMed: 7828303]
22. Zoghbi WA, Enriquez-Sarano M, Foster E, Grayburn PA, Kraft CD, Levine RA, Nihoyannopoulos P, Otto CM, Quinones MA, Rakowski H. Recommendations for evaluation of the severity of native valvular regurgitation with two-dimensional and Doppler echocardiography. J Am Soc Echocardiogr 2003;16:777–802. [PubMed: 12835667]
23. Kumanohoso T, Otsuji Y, Yoshifuku S, Matsukida K, Koriyama C, Kisanuki A, Minagoe S, Levine RA, Tei C. Mechanism of higher incidence of ischemic mitral regurgitation in patients with inferior myocardial infarction: quantitative analysis of left ventricular and mitral valve geometry in 103 patients with prior myocardial infarction. J Thorac Cardiovasc Surg 2003;125:135–143. [PubMed: 12538997]
24. Levine RA, Handschumacher MD, Sanfilippo AJ, Hagege AA, Harrigan P, Marshall JE, Weyman AE. Three-dimensional echocardiographic reconstruction of the mitral valve, with implications for the diagnosis of mitral valve prolapse. Circulation 1989;80:589–598. [PubMed: 2766511]
24a. Otsuji Y, Gilon D, Jiang L, He S, Leavitt M, Roy MJ, Birmingham MJ, Levine RA. Restricted diastolic opening of the mitral leaflets in patients with left ventricular dysfunction: evidence for increased valve tethering. J Am Coll Cardiol 1998;32:398–404. [PubMed: 9708467]
25. Chiechi M, Lees W, Thompson R. Functional anatomy of the normal mitral valve. J Thorac Surg 1956;32:378–398. [PubMed: 13358125]
26. Bossuyt PM, Reitsma JB, Bruns DE, Gatsonis CA, Glasziou PP, Irwig LM, Lijmer JG, Moher D, Rennie D, de Vet HCW. Towards complete and accurate reporting of studies of diagnostic accuracy: the STARD initiative. BMJ 2003;326:41–44. [PubMed: 12511463]
27. Rusted IE, Scheifley CH, Edwards JE. Studies of the mitral valve, I: anatomic features of the normal mitral valve and associated structures. Circulation 1952;6:825–831. [PubMed: 12998105]
28. Duplessis LA, Marchand P. The anatomy of the mitral valve and its associated structures. Thorax 1964;19:221–227. [PubMed: 14143500]
29. Hueb AC, Jatene FB, Moreira LFP, Pomerantzeff PM, Kallas E, de Oliveira SA. Ventricular remodeling and mitral valve modifications in dilated cardiomyopathy: new insights from anatomic study. J Thorac Cardiovasc Surg 2002;124:1216–1224. [PubMed: 12447190]
30. Rabkin-Aikawa E, Aikawa M, Farber M, Kratz JR, Garcia-Cardena G, Kouchoukos NT, Mitchell MB, Jonas RA, Schoen FJ. Clinical pulmonary autograft valves: pathologic evidence of adaptive remodeling in the aortic site. J Thorac Cardiovasc Surg 2004;128:552–561. [PubMed: 15457156]

31. Aikawa E, Whittaker P, Farber M, Mendelson K, Padera RF, Aikawa M, Schoen FJ. Human semilunar cardiac valve remodeling by activated cells from fetus to adult: implications for postnatal adaptation, pathology, and tissue engineering. Circulation 2006;113:1344–1352. [PubMed: 16534030]
32. Paruchuri S, Yang J-H, Aikawa E, Melero-Martin JM, Khan ZA, Loukogeorgakis S, Schoen FJ, Bischoff J. Human pulmonary valve progenitor cells exhibit endothelial/mesenchymal plasticity in response to vascular endothelial growth factor-A and transforming growth factor-β2. Circ Res 2006;99:861–869. [PubMed: 16973908]
33. Grande-Allen KJ, Griffin BP, Ratliff NB, Cosgrove DM III, Vesely I. Glycosaminoglycan profiles of myxomatous mitral leaflets and chordae parallel the severity of mechanical alterations. J Am Col Cardiol 2003;42:271–277.
34. Armstrong EJ, Bischoff J. Heart valve development: endothelial cell signaling and differentiation. Circ Res 2004;95:459–470. [PubMed: 15345668]
35. Ng CM, Cheng A, Myers LA, Martinez-Murillo F, Jie C, Bedja D, Gabrielson KL, Hausladen JMW, Mecham RP, Judge DP, Dietz HC. TGF-β-dependent pathogenesis of mitral valve prolapse in a mouse model of Marfan syndrome. J Clin Invest 2004;114:1586–1592. [PubMed: 15546004]
36. Sugi Y, Yamamura H, Okagawa H, Markwald RR. Bone morphogenetic protein-2 can mediate myocardial regulation of atrioventricular cushion mesenchymal cell formation in mice. Dev Biol 2004;269:505–518. [PubMed: 15110716]
37. Kunzelman KS, Quick DW, Cochran RP. Altered collagen concentration in mitral valve leaflets: biochemical and finite element analysis. Ann Thorac Surg 1998;66:s198–s205. [PubMed: 9930448]
38. Quick DW, Kunzelman KS, Kneebone JM, Cochran RP. Collagen synthesis is upregulated in mitral valves subjected to altered stress. ASAIO J 1997;43:181–186. [PubMed: 9152488]
39. Willems IE, Havenith MG, Smits JF, Daemen MJ. Structural alterations in heart valves during left ventricular pressure overload in the rat. Lab Invest 1994;71:127–133. [PubMed: 8041112]
40. Thubrikar MJ, Labrosse MR, Zehr KJ, Robicsek F, Gong GG, Fowler BL. Aortic root dilatation may alter the dimensions of the valve leaflets. Eur J Cardiothorac Surg 2005;28:850–855. [PubMed: 16275009]
41. Ku C-H, Johnson PH, Batten P, Sarathchandra P, Chambers RC, Taylor PM, Yacoub MH, Chester AH. Collagen synthesis by mesenchymal stem cells and aortic valve interstitial cells in response to mechanical stretch. Cardiovasc Res 2006;71:548–556. [PubMed: 16740254]
42. Dobre M, Koul B, Rojer A. Anatomic and physiologic correction of the restricted posterior mitral leaflet motion in chronic ischemic mitral regurgitation. J Thorac Cardiovasc Surg 2000;120:409–411. [PubMed: 10917964]
43. Rendon F, Aramendi JI, Rodrigo D, Baraldi C, Martinez P. Patch enlargement of the posterior mitral leaflet in ischemic regurgitation. Asian Cardiovasc Thorac Ann 2002;10:248–250. [PubMed: 12213750]
44. Langer F, Rodriguez F, Cheng A, Ortiz S, Nguyen TC, Zasio MK, Liang D, Daughters GT, Ingels NB, Miller DC. Posterior mitral leaflet extension: an adjunctive repair option for ischemic mitral regurgitation? J Thorac Cardiovasc Surg 2006;131:868–877. [PubMed: 16580446]
45. Nielsen SL, Nygaard H, Fontaine AA, Hasenkam JM, He S, Andersen NT, Yoganathan AP. Chordal force distribution determines systolic mitral leaflet configuration and severity of functional mitral regurgitation. J Am Coll Cardiol 1999;33:843–853. [PubMed: 10080490]

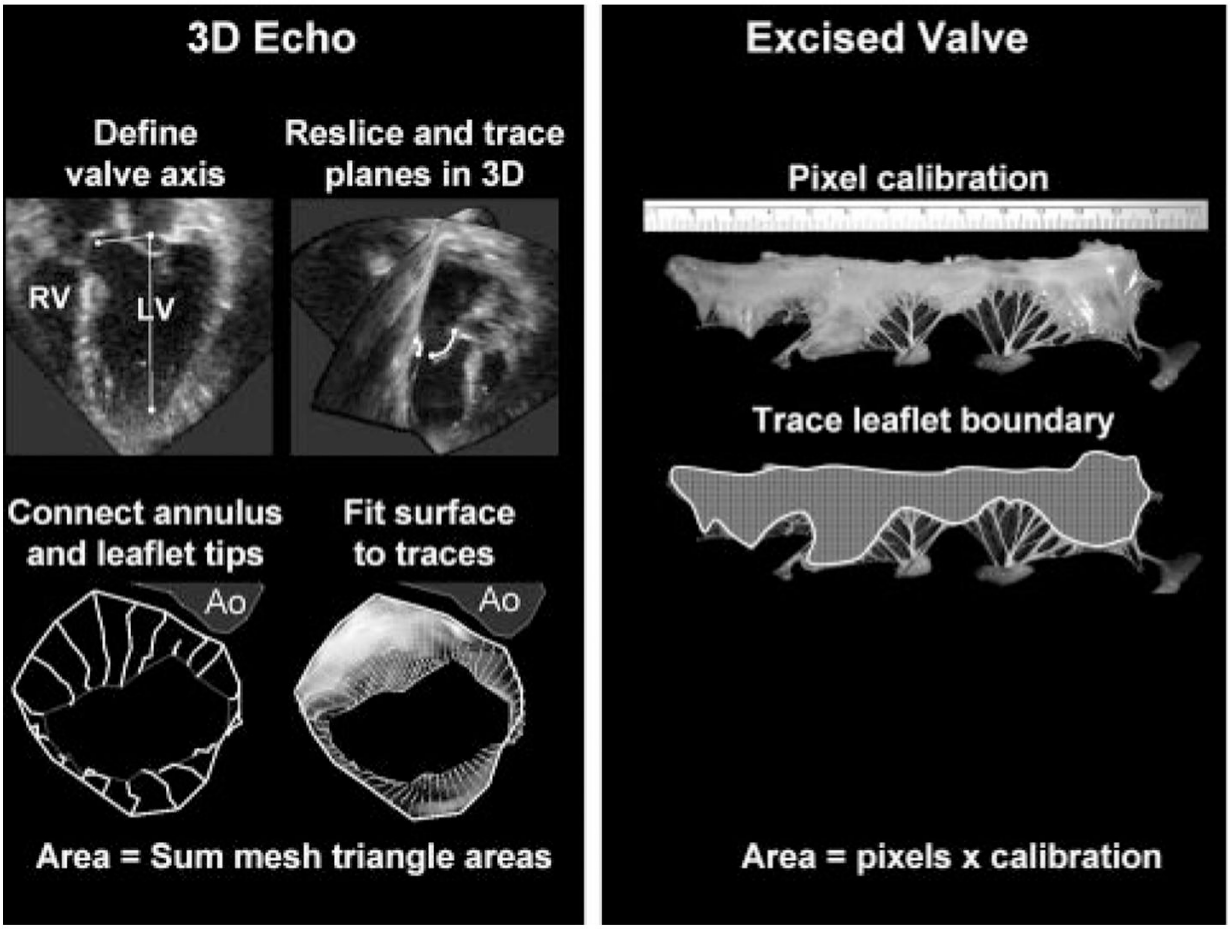

Figure 1.
Method of mitral leaflet area measurement (left) showing leaflet reconstruction in a normal beating sheep heart. The area measurement of the explanted valve from the same sheep is shown (right). RV indicates right ventricle; Ao, aorta.

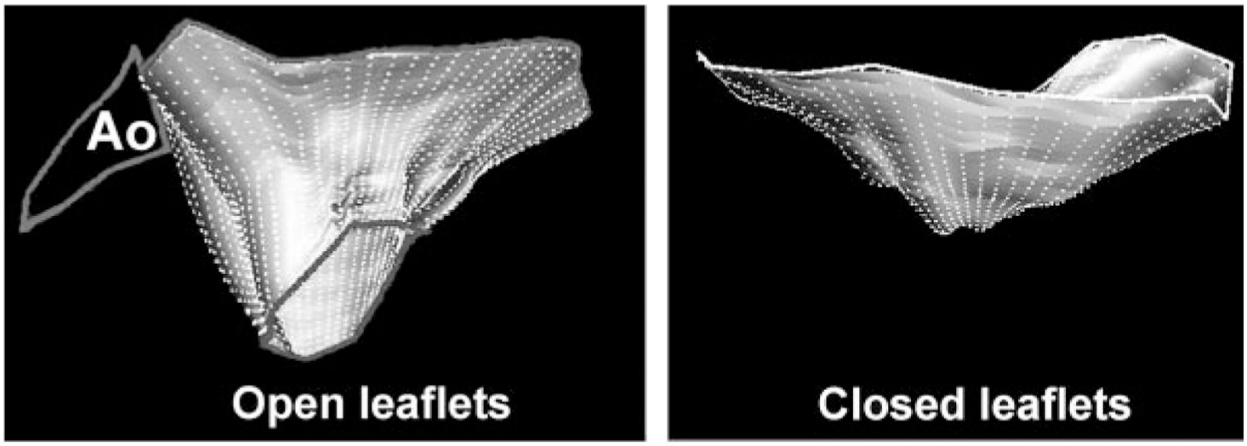

Figure 2.
Three-dimensional reconstructions of total mitral leaflet area in diastole (left) and systolic leaflet closure area (right) in a patient with FMR and both systolic and diastolic leaflet tethering.[24a] Ao indicates aorta; the left atrium is above, LV below, anterior leaflet to the left.

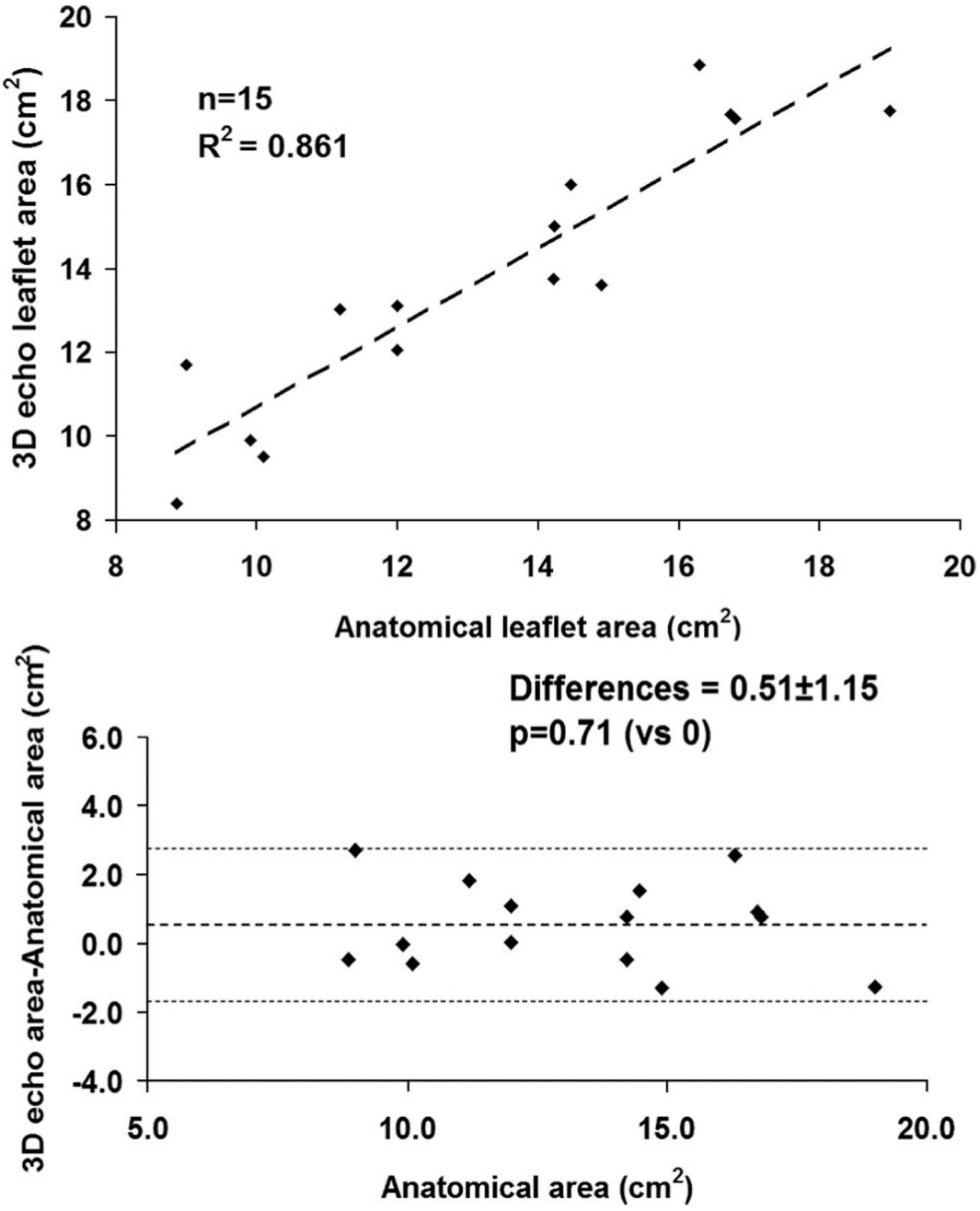

Figure 3.
Validation study of 3D echocardiography vs anatomic leaflet area in 15 normal sheep. Linear correlation (top) and Bland-Altman residual analysis (bottom) are shown.

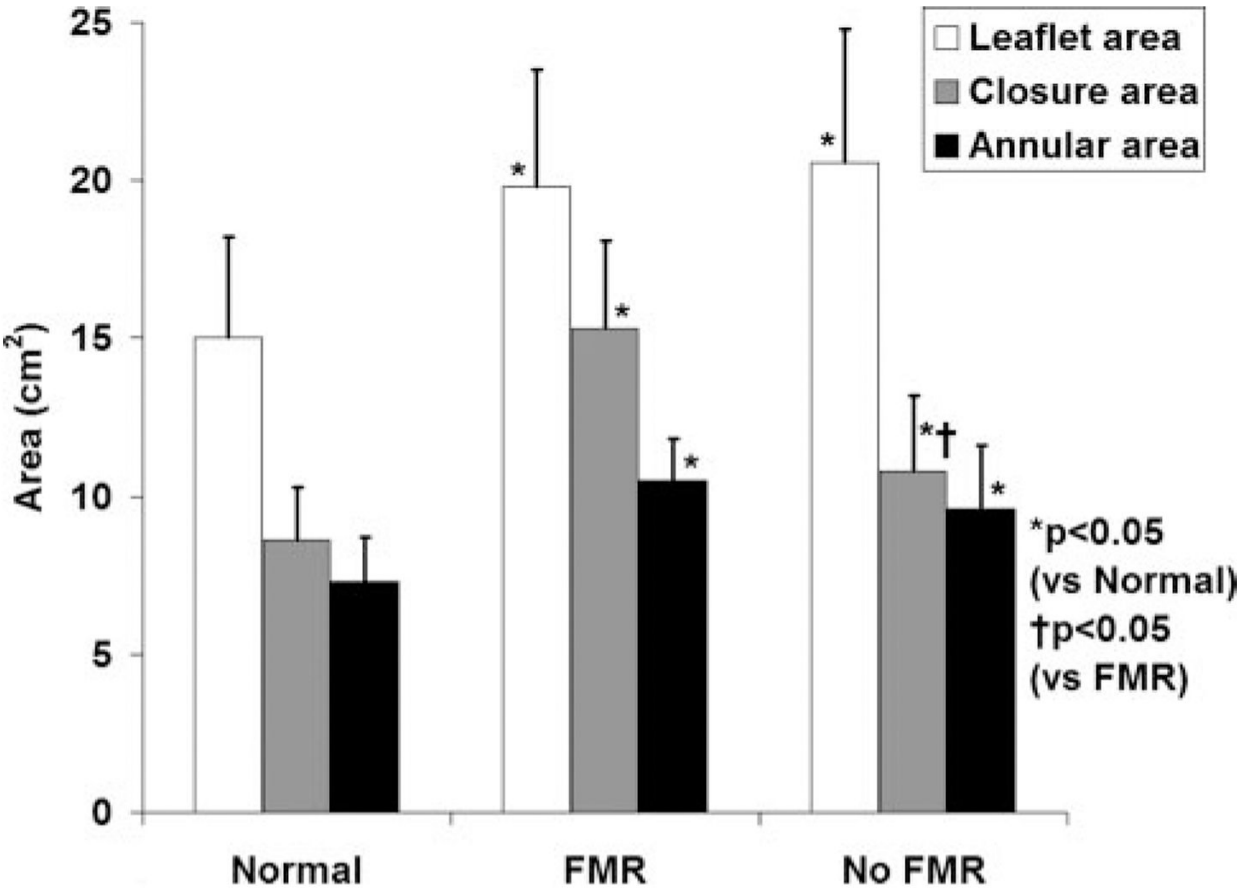

Figure 4.
Annular and leaflet areas in different patient groups.

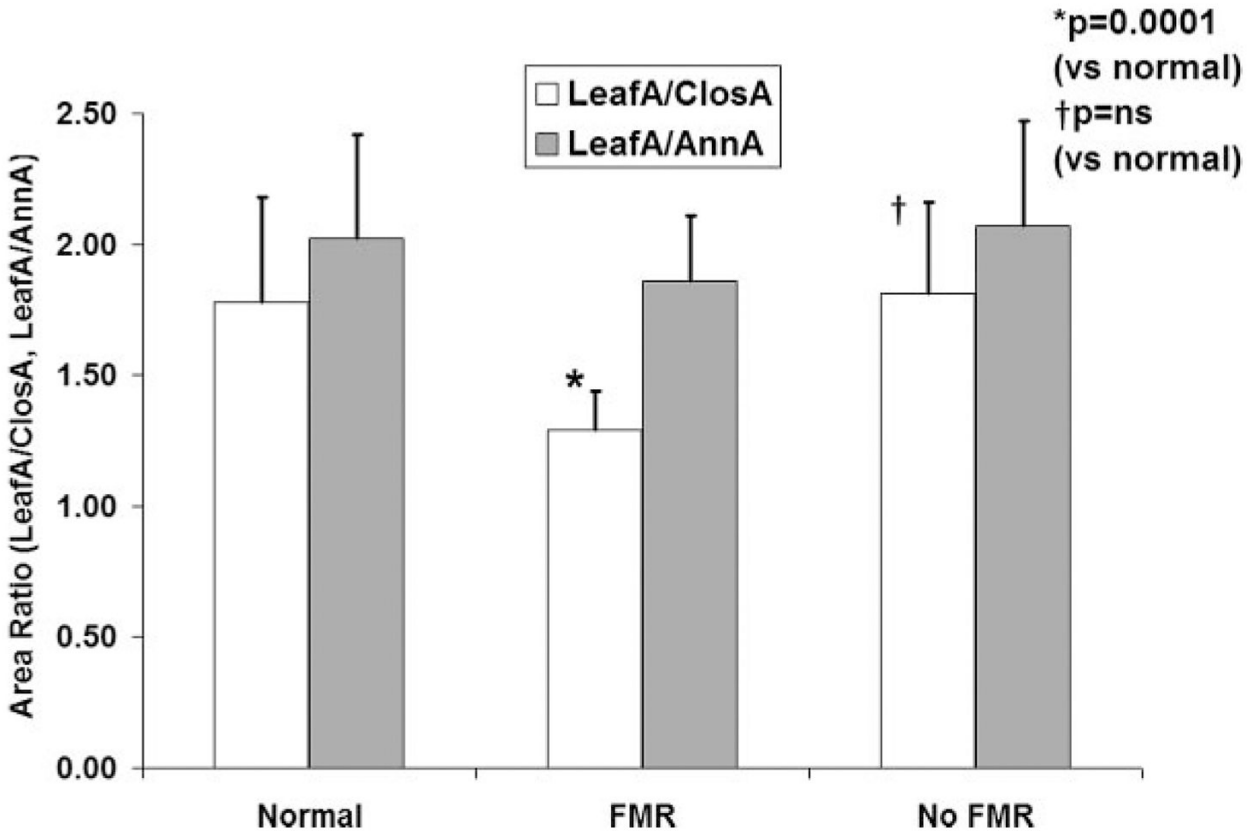

Figure 5.
Mitral leaflet area (LeafA) adjusted for closure area (ClosA) and annular area (AnnA) in different patient groups. NS indicates not significant.

Table 1

Patient Demographic Characteristics and Basic Echocardiography

	Normal (n=20)	FMR (n=29) (IWMA n=16, DCM n=13)	No MR (n=31) (IWMA n=14, DCM n=17)
Age, y†	53±18	60±17	55±15
Female gender, n (%)†	8 (40)	9 (31)	11 (35)
BSA, m^2†	1.81±0.20	1.89±0.1	1.90±0.15
HR, bpm	68±9	75±12*	78±13*
SBP, mm Hg†	120±14	117±19	123±23
DBP, mm Hg†	66±12	65±11	68±11
EF, %	60±7	33±9*	38±9*‡
EDV, mL	82±30	155±28*	125±30*‡
ESV, mL	34±17	109±32*	80±28*‡
PJW, cm	0.05±0.08	0.55±0.12*	0.15±0.10§
Tethering distance, cm	3.45±0.43	4.20±0.45*	4.00±0.45*‡
Diastolic annular area, cm^2	7.5±0.8	10.4±1.3*	9.9±2.0*‡

BSA indicates body surface area; HR, heart rate; SBP, systolic blood pressure; DBP, diastolic blood pressure; EDV, end-diastolic volume; ESV, end-systolic volume; and PJW, proximal jet width.

Values are expressed as mean±SD.

*P< 0.05 vs normal group.

†No statistically significant difference among groups (P=NS).

‡No statistically significant difference between patients with and without MR (P=NS).

§P<0.05 for MR vs no MR.

Table 2

Mitral Valve Dimensions in Patients With Normal Hearts, IWMA, and DCM, With and Without MR

	Normal (n=20)	IWMA–MR (n=16)	IWMA–No MR (n=14)	DCM–MR (n=13)	DCM–No MR (n=17)
AL length, mm†	2.43±0.34	2.65±0.29	2.53±0.40	2.75±0.40	2.41±0.19
PL length, mm†	1.14±0.15	1.36±0.20	1.38±0.18	1.23±0.21	1.27±0.09
AL thickness, mm	1.59±0.21	2.05±0.20*	1.71±0.21§	2.22±0.30*	1.95±0.31*
PL thickness, mm	1.66±0.21	2.14±0.22*	1.72±0.22§	2.21±0.25*	2.04±0.30*
Total valvular area, cm^2	15.0±2.3	19.6±2.5*	18.6±2.5*‡	20.2±2.3*	22.2±2.0*§
Diastolic annular area, cm^2	7.5±0.8	10.4±0.8*	8.4±0.9§	10.5±0.9*	11.0±1.2*‡

AL indicates anterior leaflet, PL, posterior leaflet.

*$P< 0.05$ vs normal.

†No statistically significant difference among groups (P=NS).

‡No statistically significant difference between patients with and without MR (P=NS) within the IWMA or DCM patient groups.

§$P< 0.05$ for MR vs no MR within the IWMA or DCM groups.

Table 3

Logistic Regression: Probability of Developing Moderate to Severe MR in This Patient Sample

	Univariate Logistic Regression		Multiple Variable Logistic Regression*	
Variable	**OR (95% CI)**	***P***	**OR (95% CI)**	***P***
Patient group DCM vs IWMA	3.95 (1.8–9.7)	0.003	1.7 (0.5–6.5)	0.4108
EF <35%	10.8 (2.58–43.5)	0.0011	4.9 (0.3–18.0)	0.7303
Annular dilation (>9 cm^2)	12.2 (2.86–52.0)	0.0007	2.0 (0.2–18.1)	0.1
ESV >80 mL	18.5 (4.3–83.3)	0.0001	3.7 (0.3–47.0)	0.3098
Leaflet area-to–closure area ratio <1.7	35.7 (4.27–333.3)	0.001	23.2 (2.0–49.1)	0.02
Tethering length >3.9 cm	6.5 (1.72–25.0)	0.006	2.2 (0.2–23.0)	0.5225

OR indicates odds ratio; CI, confidence interval; EF, ejection fraction; and ESV, end-systolic volume.

*Wald P=0.03.